

Mn sites in cordierite – electron paramagnetic resonance, luminescence, and optical absorption analysis

GIORGIO SPINOLO¹, SARA GABRIELLI¹, VALENTINA PALANZA¹, ROBERTO LORENZI¹, MARIA CRISTINA MOZZATI², MAURO FASOLI¹, NORBERTO CHIODINI¹, BRUNO VODOPIVEC¹ and ALBERTO PALEARI^{1,*}

¹ Department of Materials Science, University of Milano-Bicocca, via Cozzi 53, 20125 Milan, Italy

² Department of Physics “Alessandro Volta”, University of Pavia, via Bassi 6, 27100 Pavia, Italy

*Corresponding author, e-mail: alberto.paleari@mater.unimib.it

Abstract: The present work reports on the investigation of oxidation states, local symmetry, and optical properties of manganese and iron species in natural cordierite ($\text{Mg, Fe}_2\text{Al}_4\text{Si}_5\text{O}_{18}$), by means of energy-dispersive X-ray fluorescence, electron paramagnetic resonance (EPR), photoluminescence (PL) and optical absorption techniques. In particular, specific EPR characteristics show the presence of distinct Mn^{2+} octahedral sites in the crystal lattice, and a small amount of Mn^{4+} ions in tetrahedral sites. The absence of EPR signal ascribable to Mn^{4+} in octahedral sites turns out to be consistent with the lack of narrow PL lines from d^3 ions in octahedral crystal field (CF). Evidence of Mn^{3+} in octahedral sites is instead found in steady-state and time-resolved PL measurements. EPR spectra give further details on iron site occupancy, showing the occurrence of Fe^{3+} ions in octahedral sites. Characteristics ascribable to all the identified metal species have been found in the optical absorption spectrum or in the PL excitation spectrum, as arising from the expected CF transitions of Fe^{2+} , Fe^{3+} , Mn^{2+} , Mn^{3+} , and Mn^{4+} ions. Interestingly, the results show a polarization-dependent correlation between the manganese luminescence and the pleochroic absorption band at about $17,000\text{ cm}^{-1}$. This result reveals a pleochroic contribution from the Mn^{3+} spin-allowed ${}^5\text{E} \rightarrow {}^5\text{T}_2$ transition under the visible pleochroic band attributed to $\text{Fe}^{2+}(\text{oct}) \rightarrow \text{Fe}^{3+}(\text{tet})$ transitions.

Key-words: cordierite, optical absorption, time resolved photoluminescence, electron paramagnetic resonance, X-ray fluorescence, crystal field theory.

1. Introduction

For several decades the remarkable pleochroic properties of cordierite have promoted the interest in this cyclosilicate and in the role of transition metal ions in its optical properties. The possible role of iron was investigated since the beginning, revealing the occurrence of Fe^{2+} and Fe^{3+} . Fe^{2+} ions were identified as responsible for the intense and strongly polarized Crystal Field (CF) absorption structure at about $10,000\text{ cm}^{-1}$ (Farrell & Newnham, 1967; Faye *et al.*, 1968), while the local configuration of Fe^{3+} was analyzed by means of electron paramagnetic resonance (EPR) measurements (Hedgecock & Chakravarty, 1966). Detailed studies were devoted to the identification of the sites inside the cordierite structure where Fe^{2+} and Fe^{3+} ions are located. Several works definitely assessed that iron ions are mainly located in octahedral sites as Fe^{2+} ions, whereas tetrahedral sites, and probably the structural channels too, may arrange a residual quantity of Fe^{2+} and Fe^{3+} ions (Goldman *et al.*, 1977; Geiger *et al.*, 2000a; Taran & Rossman, 2001). The non negligible probability of finding Fe^{2+} and Fe^{3+} ions in nearby octahedral and

tetrahedral sites suggested the early proposed and currently accepted assignment of the pleochroic optical absorption band at $17,000\text{ cm}^{-1}$ to Inter Valence Charge Transfer (IVCT) transitions $\text{Fe}^{2+}(\text{oct}) \rightarrow \text{Fe}^{3+}(\text{tet})$ (Faye *et al.*, 1968). The detailed investigation of other possible absorption contributions in the visible spectrum from other chromophoric metal species co-existent with Fe^{2+} and Fe^{3+} is instead still lacking, specifically concerning the contribution expected from Mn^{2+} and other possible oxidation states of manganese. Indeed, the available analytical data on cordierite samples, even of very different provenance, often reveal several hundred ppm of manganese together with iron (Farrell & Newnham, 1967; Faye *et al.*, 1968; Goldman *et al.*, 1977; Geiger *et al.*, 2000b; Khomenko *et al.*, 2001), confirmed by early and more recent EPR studies reporting the observation of intense Mn^{2+} resonances (Hedgecock & Chakravarty, 1966; Geiger & Grams, 2003), which are ubiquitous in cordierite. Nevertheless, the possible manganese sites and oxidation states in cordierite, with the related consequences in the optical absorption spectrum, were not analyzed in detail. More generally, the CF transitions of the detected metal

species – either iron or manganese – have not yet been fully identified. Except for the spin-allowed transition of Fe^{2+} in pseudo-octahedral sites, responsible for the absorption structure at about $10,000\text{ cm}^{-1}$, the other crystal field transitions of Fe^{2+} , Fe^{3+} , and manganese ions have never been accounted for, leaving the interpretation of the whole optical absorption of cordierite not yet fully defined.

Aim of our present work is to identify the possible oxidation states and crystallographic sites of manganese ions in cordierite and to contribute to the interpretation of the optical properties of this system. Here we report an analysis of the optical absorption transitions of the occurring metal ions by means of a multiple experimental approach, which combines all available information and new experimental data from complementary techniques. Luminescence and paramagnetic resonance data are here analyzed to obtain the essential information on the oxidation states of the identified metal species. Then, the CF transitions of the detected Fe and Mn ions are identified in the optical absorption spectrum. This analysis also provides a clear-cut indication, based on the correlation between the Mn^{3+} luminescence excited within the pleochroic band and the polarization dependence of the band itself, that Mn species give rise to optical absorption contributions underlying the pleochroic absorption band.

2. Experimental details

Samples of cordierite, from Madagascar, were cut and polished as slabs $5 \times 5\text{ mm}$ wide and $0.5\text{--}5\text{ mm}$ thick, according to the range of absorption coefficient to be explored. Different slabs were obtained with the normal to the main surface directed along the three crystal axes c (yellow α section), a (blue γ section), and b (pale blue β section). The presence of inclusions was controlled under the optical microscope. Few small (about $10\text{ }\mu\text{m}$ in size) crystalline inclusions were revealed (identified as pyrophyllite from Raman spectra) together with films of fluid inclusions, not further identified.

Quantitative information on transition metal ions was obtained from elemental analysis performed by means of energy dispersive X-ray fluorescence (ED-XRF) using a BRUKER instrument, model ARTAX equipped with X-ray source with Mo target (50 kV, 1 mA) and a lateral resolution of 0.65 mm , after a calibration procedure carried out by comparison with the NIST 612 reference. Particularly long exposure time (500 s) was adopted in order to detect also minor contaminations up to a detection limit of about 10 ppm.

Absorption spectra were obtained by means of a PERKIN ELMER double beam spectrophotometer, model LAMBDA 950, operating in the range between $3.3\text{ }\mu\text{m}$ and 190 nm (spectral bandwidth of $0.2\text{--}20$ or $0.05\text{--}5\text{ nm}$ in the $1.0\text{--}3.3\text{ }\mu\text{m}$ and $190\text{--}1,000\text{ nm}$ ranges, respectively), corresponding to the energy region $3000\text{--}52,000\text{ cm}^{-1}$. Energy is expressed here and throughout the paper in wavenumber for an easy comparison with literature data and crystal field diagrams. Low-temperature

spectra were obtained using a GALILEO cryocooler operating in the $10\text{--}300\text{ K}$ range. Polarized spectra were obtained by using the Glan-Taylor type polarizers supplied with the spectrophotometer.

The EPR experiments were conducted using a BRUKER spectrometer in X-band (9.4 GHz) at 300 K, 18 mW of microwave power, 0.05 mT of modulation field, in condition of absence of saturation effects, for magnetic field ranging from 5 mT to 0.65 T. The angular dependence of the resonance fields of the paramagnetic species was investigated rotating the crystal around a direction approximately parallel to the [021] direction with the static magnetic field orthogonal to this direction. The concentration N of paramagnetic ions was estimated by comparison with the intensity I_s of the EPR signal of the VARIAN Strong Pitch standard ($g_s = 2.0028$, $N_s = 61,015$ spins, $S_s = 1/2$) in identical experimental conditions (modulation field amplitude, microwave power, and gain) and taking into account signal amplitude I , peak-to-peak linewidth Δ (compared with the linewidth Δ_s of the standard sample), signal multiplicity due to fine and hyperfine splitting, spin S , g -value, lineshape factor F (about 1.6, 3.6, 5.46 for Gaussian, Lorentzian and for the pitch standard of spin concentration, respectively), and sample mass, according to (Wertz & Bolton, 1972)

$$N = N_s \frac{[I\Delta^2 F g_s^2 S_s(S_s + 1)]}{[I_s \Delta_s^2 F_s g_s^2 S(S + 1)]}$$

with a final uncertainty of about 50 %.

Light-emission properties of the impurity species were investigated by means of photoluminescence (PL) data collected at 300 K. Measurements were performed by exciting at two different wavelengths with polarized excitation by using the 488 nm Ar ion laser line and the 633 nm line of a He-Ne laser (at $20,492$ and $15,978\text{ cm}^{-1}$ respectively) and detecting the signal by a JOBIN-YVON spectrometer equipped with a 300 grooves/mm grating and a CCD detector with a final spectral resolution of about 0.36 nm . In order to evaluate the role of inclusions in the macroscopic luminescence response, photoluminescence measurements were also performed by means of the confocal optics of a LABRAM DILOR spectrometer equipped with an OLYMPUS microscope, by exciting and selectively detecting in backscattering configuration the light emission of inclusions embedded in the crystals. Time-resolved measurements were performed exciting at 488 nm and chopping the excitation beam at a frequency of 50 Hz (pulse rise time $20\text{ }\mu\text{s}$), using a photomultiplier and an oscilloscope to detect the signal. The excitation pattern of the identified luminescence was analyzed by using a homemade system composed by a GEMINI 180 and a MicroHR (JOBIN-YVON) as excitation (band pass of 1.2 nm) and emission (10 nm) monochromators, respectively, and featuring a liquid nitrogen-cooled CCD (Symphony, JOBIN-YVON) as a detection system. A 450 W Xenon lamp (JOBIN-YVON) was used as excitation source. All the spectra were corrected for excitation intensity and detection response.

3. Results

3.1. EDXRF elemental analysis

The EDXRF analysis of the transition metal concentrations in several points of the investigated samples (cut from the same crystal) shows homogeneous results. The detected metal species are Fe and Mn, with concentration of $22,000 \pm 100$ ppm and 440 ± 20 ppm in weight, respectively (see Table 1). No evidence arises of possible minor contaminations by other impurities – such as Ti, Cr, V – even after 500 s of detection time, giving an upper limit of concentration of less than 10 ppm.

3.2. Optical absorption spectra

Figure 1 shows representative optical absorption spectra of the investigated cordierite samples in the $6700\text{--}30,000\text{ cm}^{-1}$ region, collected with unpolarized light and with beam direction parallel to the c , b , and a crystal axis (α , β , and γ curves in Fig. 1). Large intensity variations as a function of the crystal orientation are observed in the composite absorption

Table 1. Concentration (ppm in weight) of metal species and ions from EDXRF and EPR data.

	[Fe]	[Mn]	[Mn ²⁺]	[Mn ³⁺]	[Mn ⁴⁺]
EDXRF	22,000 (100)	440 (20)			
EPR			200 (100)		40 (20)
Calculated				200 (100)	

Notes: The [Mn³⁺] content is calculated by subtracting EPR from EDXRF data. Uncertainty is reported in brackets.

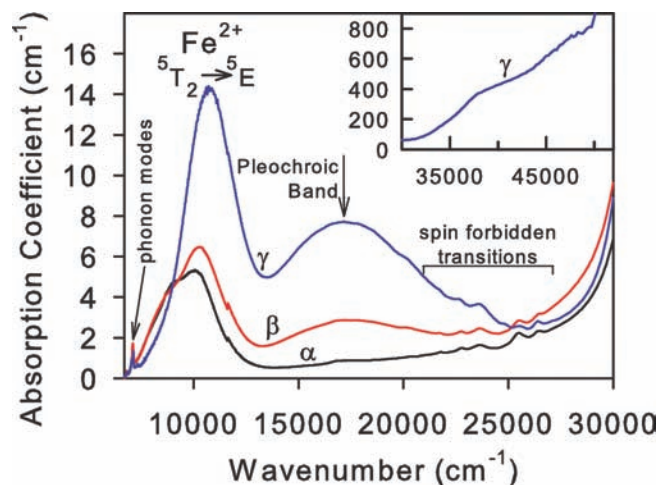


Fig. 1. Absorption spectra of cordierite in the $6700\text{--}30,000\text{ cm}^{-1}$ range, taken at 300 K obtained with unpolarized light entering different crystal faces, with the beam direction parallel to the c -axis (α section), b -axis (β section), and a -axis (γ section) of the crystal. Inset: spectrum taken at 20 K, with unpolarized light, on samples with reduced thickness, in the high-energy and high-intensity spectral region.

at $8000\text{--}12,000\text{ cm}^{-1}$ and in the broad structure centered at $17,000\text{ cm}^{-1}$, known as pleochroic band. Sharp peaks below 8000 cm^{-1} belong to the phonon spectrum of the material. These peaks correspond to combinations and overtones of vibrations of H₂O, similarly to those already studied in the varieties of beryl and assigned to water molecules trapped in the channels of the structure (Goldman *et al.*, 1977). Inset in Fig. 1 shows the high energy and high absorption portion of the spectrum in the $30,000\text{--}47,000\text{ cm}^{-1}$ range, collected on samples with 0.1 mm of thickness.

Other weak peaks are detected from $17,000$ to $27,000\text{ cm}^{-1}$, particularly evident when the intensity of the strongly polarized pleochroic band is minimized. An expanded view of this spectral region at 20 K, useful for identifying possible contributions from spin-forbidden transitions of the metal species, is reported in Fig. 2.

3.3. EPR spectra

The EPR spectra detected at 300 K with the magnetic field in two representative orientations within the (021) crystal plane are reported in Fig. 3 and 4. In insets, the spectral regions around 330 and 140 mT (in Fig. 3) and 280 and 420 mT (in Fig. 4) are reported in expanded view, showing the details identifying the iron and manganese EPR-active configurations. Sextets from hyperfine (hf) interaction with the $I = 5/2$ nuclear spin of manganese are indicated, as well as g -values of the main iron signals. Two values of manganese hf-splitting are observed in the identified sextets, equal to 8.9–9.0 mT (Fig. 3) and 7.5 mT (Fig. 4). Manganese signals with the smaller hf splitting are much weaker than the other Mn resonances, approximately by a factor 30, but with a slightly larger linewidth. Amplitude, linewidth, and multiplicity of the signals give the way to estimate the fraction of manganese occurring as Mn²⁺ and

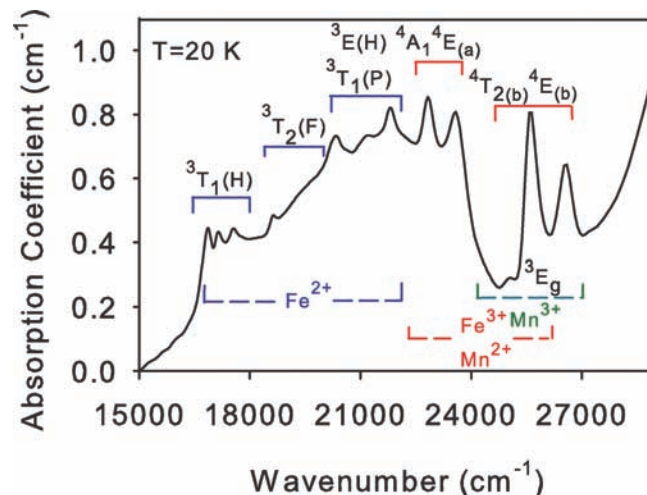


Fig. 2. Unpolarized absorption spectrum taken at 20 K parallel to the c crystal axis, showing the detailed structure arising from the weak spin-forbidden transitions of the detected metal ions. Labels refer to the energy regions expected for the excited levels of the indicated ions, according to previous works.

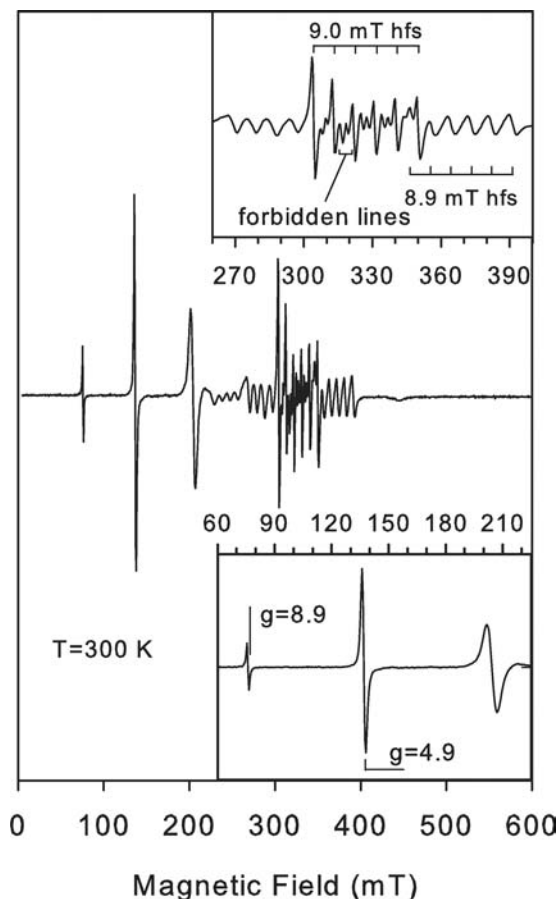


Fig. 3. EPR spectrum at 300 K with the magnetic field in the (021) plane. Upper inset: expanded view of the spectral region at $g \sim 2$, showing different types of Mn^{2+} spectra. Sextets from hyperfine interaction with the Mn nuclear magnetic spin are also shown. Lower inset: expanded view of the spectral region of the Fe^{3+} spectrum at high g values.

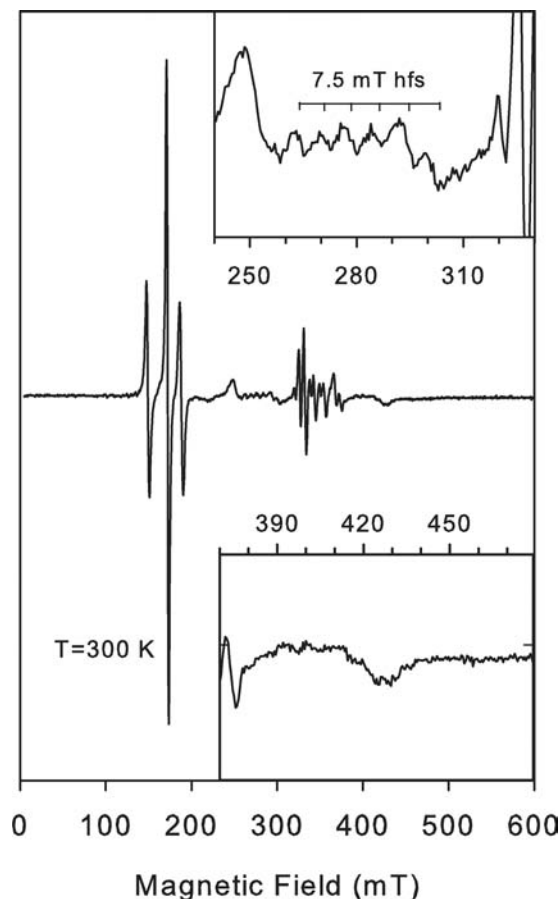


Fig. 4. EPR spectrum at 300 K with the magnetic field in the (021) plane, rotated by 75° with respect to Fig. 3. Insets: expanded views of the spectral region at $g \sim 2$, showing a weak six fold hyperfine structure of 7.5 mT identifying the Mn^{4+} resonance (upper inset) and an unstructured resonance not attributable to tetrahedrally coordinated Fe^{3+} ions (lower inset).

Mn^{4+} ionic species, as reported in Table 1 together with the values obtained from ED-XRF analysis.

The angular variations of the resonance fields of the EPR signals are shown in Fig. 5a, b for iron and manganese signals, respectively. Resonance fields are discriminated according to the presence and splitting value of the hf structure. Continuous lines in Fig. 5a are the calculated dependence of the resonance fields obtained from the projection in the magnetic field direction of the g -tensors with effective principal values $g_x^a = 3.683$, $g_y^a = 3.232$, $g_z^a = 5.084$, and $g_x^b = 3.683$, $g_y^b = 9.074$, $g_z^b = 1.25$, describing Zeeman transitions of the Fe^{3+} configuration in X-band within two of the three doublets separated by zero-field splitting (Hedgecock & Chakravarty, 1966). The local x -axis is parallel to the crystal c -axis, as observed by Hedgecock & Chakravarty (1966), with the z -axis forming an angle of $-\pi/6$ or $+\pi/6$ with the crystal a -axis, as expected from the twofold symmetry axes of the Al tetrahedra in (k) positions. Our data give a new estimation of g_z^b that was uncertain in the early work because of low signal intensity and Mn interference (Hedgecock & Chakravarty,

1966). The dashed line in Fig. 5a and all the curves in Fig. 5b are guides for the eyes.

3.4. Photoluminescence data

The PL emission-excitation pattern (Fig. 6) shows a single structured luminescence in the red spectral region, approximately at $14,500\text{--}15,000\text{ cm}^{-1}$, with five excitation structures at $17,500$, $21,300$, $22,700$, $24,500$, and $26,700\text{ cm}^{-1}$. Measurements performed by means of laser sources (at $15,978\text{--}20,492\text{ cm}^{-1}$) show that the emission excited within the $17,500\text{ cm}^{-1}$ band, in the spectral region of the pleochroic absorption band, depends significantly on the direction of the exciting beam polarization (Fig. 7). Specifically, the PL band is more intense when the polarization of the excitation within the pleochroic absorption band is directed so as to give a larger absorption. Time resolved PL measurements (Fig. 8) give a decay time of about 5 ms, varying from 5.0 to 5.2 ms rotating the polarization within the plane orthogonal to the c -axis from the condition of maximum to minimum PL intensity,

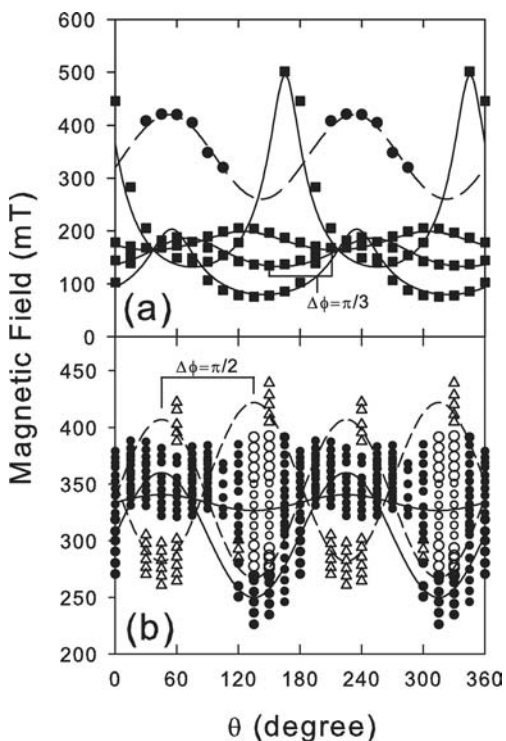


Fig. 5. Angular dependence of the resonance fields of (a) Fe^{3+} and (b) manganese spectra, with the magnetic field in the (021) plane ($\pm 5^\circ$). In (a), resonances from Fe^{3+} in tetrahedral sites, with a $\pi/3$ phase difference, and resonances with π periodicity from octahedral sites are indicated by squares and by circles, respectively. In (b), Mn^{4+} and Mn^{2+} resonances, discriminated by the hf splitting value, are indicated by triangles and circles, respectively. Filled and open circles with different size refer to Mn^{2+} signals with different line-width. Curves in (b) are guides for the eyes.

respectively. Possible spurious contributions to the $14,500\text{ cm}^{-1}$ PL band from the optical activity of inclusions is ruled out, as evidenced by PL spectra collected through confocal optics focused on inclusions, showing the known pyrophyllite emission band in the region between $16,000$ and $19,000\text{ cm}^{-1}$. This emission is superimposed and definitely different to the main PL activity, and it is not observed outside the inclusions (inset in Fig. 7).

4. Discussion

In the following discussion, we first identify the types of transition metal ions occurring in the investigated crystal, considering analytical data, EPR data, and light emission properties. Then, in the next sections, we systematically allocate the expected crystal field transitions of the identified ions in the absorption spectrum, from the spin-forbidden to the spin-allowed transitions.

4.1. Metal species and their oxidation state

4.1.1. Analytical data

The absence of ED-XRF signal from metal species different from Fe and Mn fixes the concentration of other metal cations in few ppm at most. This result allows us to rule out any relevant contribution to the optical absorption spectrum from other transition metal ions than Fe and Mn. In fact, the most intense spin-allowed absorption features expected from other ions would have intensity more than three orders of magnitude lower than the absorption band at about $10,000\text{ cm}^{-1}$ caused by spin allowed transitions of Fe^{2+} ions. Looking at manganese, the identification of its

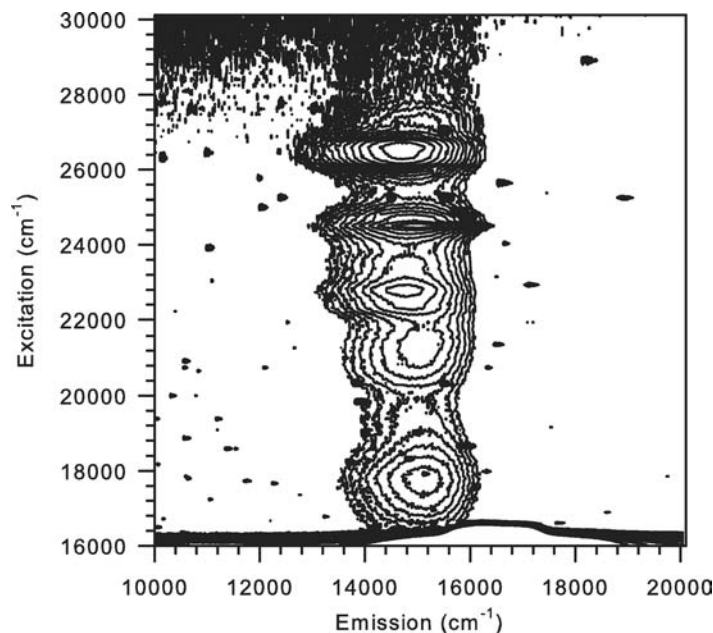


Fig. 6. Contour plot of photoluminescence signal intensity in cordierite as a function of the excitation energy, taken at 300 K with unpolarized light.

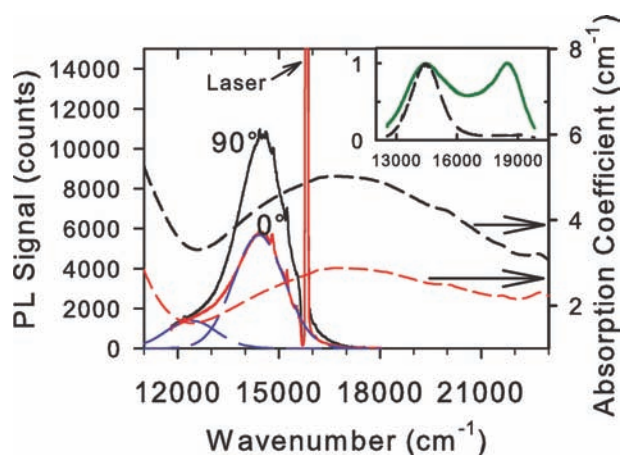


Fig. 7. Photoluminescence spectra excited by the 633 nm line of a He-Ne laser at two orthogonal polarization directions minimizing and maximizing (0° and 90° , respectively) the pleochroic absorption (dashed curves). Analysis in Gaussian components of the structured band is also shown. Inset: PL spectra collected in confocal configuration (focal depth about $10\ \mu\text{m}$) focusing an inclusion (full line) and just outside it (dashed line).

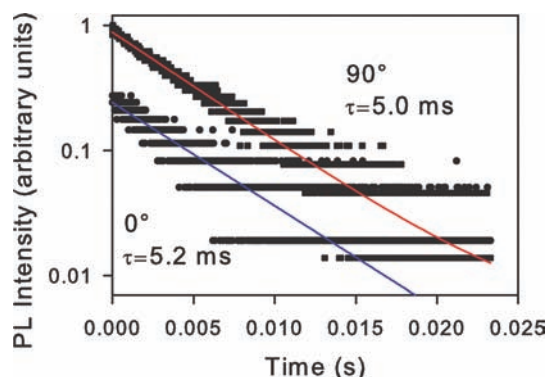


Fig. 8. Time decay of PL at $15,000\ \text{cm}^{-1}$ taken at 300 K by exciting at 488 nm at two orthogonal orientations of the excitation polarization.

role in the absorption spectrum has to pass through the identification of its oxidation states really occurring in the crystal. The combined analysis of EPR and luminescence data is crucial to achieve a reliable interpretation of the system. The experimental data in Table 1, giving the total iron and manganese concentration from ED-XRF analysis and Mn^{2+} and Mn^{4+} concentrations through EPR spectra, allow to determine the manganese oxidation states in the investigated material. In particular, the Mn^{3+} content is obtained by subtracting EPR data of Mn^{2+} and Mn^{4+} concentration from the EDXRF value of Mn content, supposing negligible other oxidation states of manganese.

4.1.2. EPR active Fe and Mn oxidation states

The narrow EPR signals without hf structure in Fig. 3 and 4, at magnetic field ranging from 70 to 200 mT, reveal the presence of Fe^{3+} ions. The dependence of the EPR spectrum on the direction of the magnetic field, as shown in Fig. 5a,

allows us to distinguish three Fe^{3+} spectra – two spectra differing in phase by $\pi/3$, each composed by two resonances in the range of g -value between 1.2 and 9 (squares in Fig. 5a), and a spectrum composed by a single resonance with a π -periodicity in the g -range 1.6–2.6 (circles in Fig. 5a). The spectra at large g -values comes from transitions within different zero-field split states of Fe^{3+} substitutional for Al^{3+} in tetrahedral (k) sites, according to the work of Hedgecock & Chakravarty (1966). The third spectrum at g -value around $g = 2$ (lower inset in Fig. 4) was not observed in the early study, probably for a lower content of iron impurities. This new spectrum reveals the presence of different Fe^{3+} sites in the crystal. The g -values in the 1.6–2.6 range are compatible with Fe^{3+} in relatively high symmetry sites, and suggest the presence of Fe^{3+} in the distorted octahedral M sites of cordierite.

Besides Fe^{3+} ions, the EPR spectra show clear evidence of EPR-active manganese ions in two different oxidation states, identifiable by distinct hf structures caused by the $I = 5/2$ nuclear spin of the ^{55}Mn nucleus. Hyperfine sextets with hf splitting of about 9 mT (inset in the upper side of Fig. 3) indicate the presence of Mn^{2+} ions, while a sextet with hf splitting of 7.5 mT (inset in the upper side of Fig. 4) is a clearcut evidence of the co-existence of Mn^{4+} in the crystal (Rakhimov *et al.*, 2004). However, the low signal intensity with respect to the other Mn signals allows us to estimate that $[\text{Mn}^{4+}]$ should be lower than $[\text{Mn}^{2+}]$ by approximately a factor 5. The Mn^{4+} spectrum is composed by two signals with a $\pi/2$ -phase difference. This result rules out tetrahedral (k) sites, whereas it would be consistent with Mn^{4+} ions in tetrahedral b sites (T₁6 tetrahedra). This attribution would be compatible with luminescence data that do not show the characteristic narrow doublet from d^3 configuration in octahedral environment (as Cr^{3+} in ruby).

As regards the EPR spectrum of Mn^{2+} ions, several hf structures overlap in the quite restricted 300–400 mT range of magnetic field where the $M_s = -1/2 \rightarrow +1/2$ transition gives rise to the main Mn^{2+} resonances in the spectra. Anyway, the multiplicity of signals and the presence of at least two distinct kinds of resonance lines with different line-width (see upper inset in Fig. 3), reveal more than one site occupied by Mn^{2+} ions. In fact, the net differences between the central Mn^{2+} sextet – with very narrow lines accompanied by five doublets of spin forbidden $M_1 = \pm 1$ resonances (Gunasekaran & Anbalagan, 2008) – and the two much broader sextets at its sides clearly suggest the presence of distinct sites, one of which with an efficient source of line broadening such as hf interactions with nearby ions with non-null nuclear spin. Indeed, Mn^{2+} sites adjacent to tetrahedral Al^{3+} sites (100 % nuclear spin $I = 5/2$) might give rise to such a broadened sextet.

Summarizing the information coming from EPR data, we can say that iron and manganese are present in the crystal with the EPR-active valence states Fe^{3+} , Mn^{2+} , and Mn^{4+} . The first two kinds of ions indeed occur in more than one crystallographic site and they turn out to be predominant in concentration with respect to Mn^{4+} . Besides these ions, Mn^{3+} and Fe^{2+} have also to be taken

into account. The occurrence of Fe^{2+} ions is confirmed by the characteristic intense optical absorption at about $10,000\text{ cm}^{-1}$. On the other hand, the difference between the total manganese contents and the concentration of EPR active manganese sites suggests the presence of Mn^{3+} ions. The occurrence of Mn^{3+} is indeed quite reasonable in a system with coexisting Fe^{2+} , Fe^{3+} , Mn^{2+} , and Mn^{4+} ions. Direct evidence of Mn^{3+} cannot be found in our EPR spectra because Mn^{3+} is EPR-silent in the investigated conditions (Goldberg *et al.*, 1997). Nevertheless, evidence of Mn^{3+} ions comes from luminescence data, as we show in the following section.

4.1.3. Manganese luminescence

The photoluminescence emission at $14,500\text{ cm}^{-1}$ may be attributed to manganese species. In fact, Fe^{3+} ions do not usually give luminescence activity in that spectral region, and Fe^{2+} ions, similarly to several other Jahn-Teller (JT) d^6 systems, do not show photoluminescence in oxides because of efficient non-radiative decay mechanisms (Sanz-Ortiz & Rodríguez, 2009). By contrast, Mn^{2+} and Mn^{3+} in octahedral coordination, as well as Mn^{4+} in tetrahedral sites, give rise to red photoluminescence with intensity often interesting for applications in phosphors and also for laser materials (Green & Walker, 1985; Kuck *et al.*, 1998; Williams *et al.*, 2004; Lin *et al.*, 2006).

The red luminescence of octahedrally coordinated Mn^{2+} ions usually consists of a broad band at around $14,500\text{ cm}^{-1}$, but it is sometimes detected at higher energy up to $16,500\text{ cm}^{-1}$. This luminescence is observed in several phosphors and minerals (Stevens, 1979; Green & Walker, 1985; Lin *et al.*, 2006) with an excitation spectrum usually composed of quite narrow bands from $21,000$ to $28,000\text{ cm}^{-1}$. The spectral position of the high energy excitation features in Fig. 6, from $21,000$ to $27,000\text{ cm}^{-1}$, is indeed consistent with the energy expected from Mn^{2+} transitions from the ${}^6\text{A}_1$ ground state to the excited level ${}^4\text{T}_{1g}$ ($21,000\text{ cm}^{-1}$), ${}^4\text{T}_{2g}$ ($22,700\text{ cm}^{-1}$), ${}^4\text{E}_g$, ${}^4\text{A}_1$ ($24,500\text{ cm}^{-1}$), and ${}^4\text{T}_{2g}$ ($27,000\text{ cm}^{-1}$). On the other hand, Mn^{2+} cannot relevantly contribute to the observed red PL band excited in the region of the pleochroic absorption, since the low energy photons from the $15,978\text{ cm}^{-1}$ line of the excitation laser source do not efficiently promote Mn^{2+} ions to the excited level.

Detailed studies on synthetic Mn-doped garnets (Kuck *et al.*, 1998) showed instead that Mn^{3+} ions in pseudo-octahedral environment in oxides give rise to a quite broad and structured red luminescence at about $15,000$ – $16,000\text{ cm}^{-1}$, similar to that we observed in cordierite. The decay time of this emission falls in the ms domain in all the Mn-doped crystals investigated, comparable with the experimental lifetime of about 5 ms we have measured in cordierite. Several other features of the $14,500\text{ cm}^{-1}$ luminescence are indeed an evidence of Mn^{3+} ions in the crystal, such as the composite shape. Specifically, the presence of a low-energy component peaked at $12,400\text{ cm}^{-1}$ is consistent with the expected effect of Jahn Teller stabilization resulting in a splitting of the t_{2g} electronic wavefunctions (Sanz-Ortiz & Rodríguez, 2009).

Mn^{4+} in tetrahedral sites may give an additional contribution to the observed red luminescence thanks to the ${}^2\text{T}_2 \rightarrow {}^4\text{T}_1$ transition, as indeed observed in some phosphors (van Ipenburg *et al.*, 1995; Williams *et al.*, 2004). The main excitation region of this luminescence lies at high energy above $30,000\text{ cm}^{-1}$, quite beyond the range of our data. However, a minor excitation band was observed just at about $21,000\text{ cm}^{-1}$, consistently with the feature in the excitation pattern in Fig. 6.

In summary, as concerns photoluminescence results, the observed $14,500\text{ cm}^{-1}$ photoluminescence is a strong evidence of manganese ions in cordierite, specifically Mn^{3+} in octahedral sites. The dependence of this luminescence as a function of the excitation polarization will be of help in the discussion of the absorption features in the next sections. In fact, this dependence will give a conclusive indication of the presence of Mn^{3+} absorption in the region of the pleochroic band.

4.2. Spin-forbidden absorption transitions

The above discussion – based on analytical, EPR, and luminescence results – gives us important indications on the optical active species we have to take into account in the interpretation of the bundle of weak and strong, narrow and broad features in the absorption spectrum of cordierite. Specifically, we expect to find contributions from Fe^{2+} (d^6), Fe^{3+} (d^5), Mn^{2+} (d^5), Mn^{3+} (d^4), and Mn^{4+} (d^3) ions.

Weak peaks are expected in the spectral region from $17,000$ to $22,000\text{ cm}^{-1}$ from spin-forbidden transitions of Fe^{2+} , namely from transitions to the ${}^3\text{T}_1(\text{H})$, ${}^3\text{T}_2(\text{F})$, ${}^3\text{T}_1(\text{P})$, and ${}^3\text{E}(\text{H})$ levels, as observed in beryl, in aqueous solutions and in halides (Pollini *et al.*, 1980; Fontana *et al.*, 2007; Spinolo *et al.*, 2007). The spectral position of these transitions corresponds well with the weak peaks we have observed in the spectral region below $22,000\text{ cm}^{-1}$ (Fig. 2).

As regards Fe^{3+} and Mn^{2+} , which are both d^5 ions, all the expected transitions in the visible region are spin forbidden and, consequently, rather weak. Looking at the details in the spectrum of Fig. 2, contributions from Fe^{3+} should be found above $22,000\text{ cm}^{-1}$, as we can argue from data in beryl, aqueous solutions and corundum (Krebs & Maisch, 1971; Fontana *et al.*, 2007; Spinolo *et al.*, 2007). Similarly, also the spin forbidden transitions of Mn^{2+} are expected at energy higher than about $23,000\text{ cm}^{-1}$, as observed in a number of salts (Lohr & McClure, 1968). In more details, the excitations to the ${}^4\text{A}_1$, ${}^4\text{E}_{(a)}$, ${}^4\text{T}_{2(b)}$ and ${}^4\text{E}_{(b)}$ levels should give rise to peaks in the $22,000$ – $30,000\text{ cm}^{-1}$ range both for Fe^{3+} and Mn^{2+} . In particular, the peaks at $25,100$ and $25,700\text{ cm}^{-1}$ correspond to the positions of ${}^4\text{T}_{2(b)}$ and ${}^4\text{E}_{(b)}$ levels, while transitions to ${}^4\text{A}_1$, ${}^4\text{E}_{(a)}$ may give rise to the double structure at $23,000$ – $23,500\text{ cm}^{-1}$. We note that the number of peaks from all these spin-forbidden transitions does not appear doubled for the simultaneous presence of two d^5 configurations belonging to Fe^{3+} and Mn^{2+} . Indeed, because of the lower Mn^{2+} concentration with respect to Fe^{3+} , only minor features are expected, supposing similar oscillator strength.

Thanks to the excitation pattern of Mn luminescence (Fig. 6) it is however possible to identify the positions of distinct Mn^{2+} contributions just above $21,000\text{ cm}^{-1}$, where there is a small bump in the absorption spectrum (Fig. 2), and at $24,500\text{ cm}^{-1}$, evidenced by a shoulder. The weak intensity of these features, compared with the other absorption peaks, shows that Mn^{2+} ions are significantly less than Fe^{3+} ions, consistently with the ratio between the estimated Fe and Mn concentrations. There are other contributions that are suggested by the PL excitation spectrum and that turn out compatible with Mn^{2+} transitions (specifically the peaks at $22,700$ and $26,700\text{ cm}^{-1}$). These contributions fall just in correspondence of well-defined absorption peaks in the region of spin-forbidden transitions. However, since it is unlikely that the intensity of these transitions be largely different from the weak absorption features at $21,000$ and $24,500\text{ cm}^{-1}$, other species probably contribute to the $22,700$ and $26,700\text{ cm}^{-1}$ peaks. Both peaks indeed lie in positions where Fe^{3+} transitions are expected (Krebs & Maisch, 1971), specifically to the ${}^4\text{A}_1$, ${}^4\text{E}_{(a)}$ and to ${}^4\text{E}_{(b)}$ levels. Furthermore, also Mn^{3+} should give rise to spin-forbidden transitions at relatively high energy, the first one being to the ${}^3\text{E}$ level. The latter transition may indeed contribute to one of the two high-energy excitation peaks at $24,510$ and $26,700\text{ cm}^{-1}$ in Fig. 6, and to the $24,000$ – $27,000\text{ cm}^{-1}$ absorption region (probably superimposed to the quite significant peaks at $25,600$ and $26,560\text{ cm}^{-1}$ due to Fe^{3+} transitions). This analysis is consistent with early data on Mn^{3+} in corundum (McClure, 1962).

All the narrow peaks in the absorption spectrum of cordierite thus find an interpretation as spin-forbidden transitions of iron, the most abundant metal species, with possible minor contributions due to Mn^{2+} ions. Contributions from Mn^{4+} spin-forbidden transitions probably lie below the experimental detection limit.

4.3. Spin-allowed absorption transitions

The main feature assignable to spin-allowed transitions of metal ions in the absorption spectrum of cordierite is the strong composite structure at about $10,000\text{ cm}^{-1}$ (Fig. 1). This feature is caused by spin-allowed excitation of the ${}^5\text{T}_2$ ground state of Fe^{2+} (d^6) in distorted octahedral environment to the Jahn-Teller split ${}^5\text{E}$ excited configurations. These transitions give rise to a strongly polarized structure with two components. At room temperature the stronger component is found at $10,750$ and the weaker one at 8700 cm^{-1} . The 2050 cm^{-1} splitting of the Jahn-Teller components is indeed rather similar to that (1900 cm^{-1}) observed in beryl-aquamarine (Spinolo *et al.*, 2007), with the barycenter of the two bands shifted about 1400 cm^{-1} at lower energy in cordierite. Concerning the other identified impurity ions, no spin-allowed transition is expected in the visible region from Fe^{3+} and Mn^{2+} d^5 ions, as we have just discussed in the previous section. By contrast, Mn^{3+} and Mn^{4+} ions – the other two metal species

identified by EPR in our cordierite sample – may contribute to the absorption spectrum through spin-allowed transitions.

The PL excitation spectrum in Fig. 6 shows that the red luminescence possesses an excitation channel at about $21,000\text{ cm}^{-1}$. This excitation was already observed in other systems with Mn^{4+} in tetrahedral coordination (van Ipenburg *et al.*, 1995; Williams *et al.*, 2004) and it is ascribable to the ${}^4\text{T}_1 \rightarrow {}^4\text{A}_2$ transition of Mn^{4+} in tetrahedral sites. The detection of this Mn^{4+} excitation suggests an absorption contribution at about $21,000\text{ cm}^{-1}$, probably hidden by the pleochroic absorption. This contribution, despite the small amount of Mn^{4+} ions, should however possess a quite large oscillator strength, as often observed for transition metal ions in tetrahedral coordination.

As regards Mn^{3+} ions in octahedral coordination, a lot of studies both on minerals and synthetic compounds agree in the identification of the main absorption band of this ion just in the visible region. The main contribution of the Mn^{3+} absorption consists in a broad polarized composite band at about $19,000$ – $21,000\text{ cm}^{-1}$, with two components arising from spin-allowed transitions from the ground ${}^5\text{E}$ state to the first excited ${}^5\text{T}_2$ level (Holmes & McClure, 1957; McClure, 1962; Kuck *et al.*, 1998; Noginov *et al.*, 1999; Padlyak *et al.*, 2006). Its intensity was observed to reach absorption coefficient values of the order of 10^{-1} – 10^0 cm^{-1} for Mn^{3+} concentration ranging from 0.5 to $2.5 \times 10^{18}\text{ cm}^{-3}$, corresponding to tens to hundreds ppm (Kuck *et al.*, 1998). Further data on Mn^{3+} in andalusite- and epidote-type minerals and other miscellaneous minerals supporting this phenomenology may be found in Smith *et al.* (1982) and Burns (1993). So, there is evidence that Mn^{3+} in pseudo-octahedral coordination displays its main optical absorption activity as a polarized band from the spin allowed ${}^5\text{E} \rightarrow {}^5\text{T}_2$ transition, with a large absorption cross section (up to 10^{-18} cm^2) and about 4000 cm^{-1} wide, but possibly split or broadened by distortions. These facts suggest that the expected $\text{Mn}^{3+}{}^5\text{E} \rightarrow {}^5\text{T}_2$ CF transition might give a polarized contribution in the pleochroic absorption region. The correlation between the visible pleochroic band and the Mn^{3+} light-emission (Fig. 7) indeed appears to support the presence of such a contribution. As a matter of fact, our PL data show that the Mn^{3+} luminescence spectrum, with the expected long lifetime, is excited within the pleochroic band with a dependence on the polarization that definitely connects it to some species contributing to the pleochroic absorption. When the polarization of the incident light beam is directed so as to maximize the pleochroic absorption – with a strong attenuation of the light intensity – the luminescence is maximized as well. This fact clearly indicates that it is not a mere spectral coincidence that the Mn^{3+} luminescent sites are excited in the same energy region of the pleochroic absorption. This correlation is instead the evidence that the excited luminescent Mn^{3+} ions and a fraction of the sites responsible for the pleochroic band do coincide. Otherwise, absorption would be competitive with the luminescence excitation and we would observe a weaker

luminescence for polarization maximizing the pleochroic absorption. This fact constitutes a clearcut evidence of a pleochroic absorption contribution in the visible region from localized transitions of manganese ions.

Nevertheless, other CF transitions can give minor contributions to the absorption in this region. Particularly some spin-forbidden transitions of Fe^{2+} , Fe^{3+} , Mn^{2+} in the 14,000–25,000 cm^{-1} energy range.

4.4. Charge transfer transitions

We complete the analysis of the optical absorption phenomenology by a discussion of the charge transfer (CT) absorption region. In inset of Fig. 1 we see the low-temperature CT spectra up to 47,000 cm^{-1} and up to 8×10^2 cm^{-1} in absorption coefficient, showing the presence of bands at 36,000 and 40,000 cm^{-1} . The spectral features in this high-energy region are very similar to that of aquamarine (Spinolo *et al.*, 2007) and olivine (Runciman *et al.*, 1973), which show absorption bands attributed to CT transitions oxygen \rightarrow Fe^{3+} . Above 46,000 cm^{-1} , after removing the polarizers, we observe a further absorption that may be due to either oxygen \rightarrow Fe^{2+} CT transition or to CT transition from oxygen to some valence state of Mn, as proposed by Noginov *et al.* (1999).

5. Conclusions

The detailed analysis of the optical activity of transition metal impurities in cordierite, starting from the analytical and spectroscopic determination of the occurring elements and their oxidation states, brings us to remark the following facts: (a) iron and manganese ions are the relevant substitutional species in cordierite, our analytical results matching and confirming all previous data in the literature; (b) Fe^{2+} ions occupy octahedral sites while Fe^{3+} ions are mainly located in tetrahedral sites, but are also found in octahedral sites; (c) Mn^{2+} in octahedral sites show distinct types of environments; (d) a small amount of Mn^{4+} ions is also found, located in tetrahedral sites; (e) all the crystal-field transitions of the detected species give rise to spectral structures identifiable in the absorption spectrum (with the aid of the PL excitation spectrum in the case of Mn sites); (f) the correlation between spectral and polarization features of Mn^{3+} luminescence and the expected spin-allowed absorption of this ion – arising from the ${}^5\text{E} \rightarrow {}^5\text{T}_2$ transition – reveals a contribution of Mn^{3+} ions to the pleochroic band at 17,000 cm^{-1} .

References

Burns, R.G. (1993): Mineralogical applications of crystal field theory. Cambridge University Press, Cambridge, UK.
 Farrell, E.F. & Newnham, R.E. (1967): Electronic and vibrational absorption spectra in cordierite. *Am. Mineral.*, **52**, 380.

Faye, G.H., Manning, G.P., Nickel, E.H. (1968): The polarized optical absorption spectra of tourmaline, cordierite, chloritoid and vivianite: ferrous-ferric electronic interaction as a source of pleochroism. *Am. Mineral.*, **53**, 1174.
 Fontana, I., Lauria, A., Spinolo, G. (2007): Optical absorption spectra of Fe^{2+} and Fe^{3+} in aqueous solutions and hydrated crystals. *Physica Status Solidi B.*, **244**, 4669–4677.
 Geiger, C.A. & Grams, M. (2003): Cordierite IV: structural heterogeneity and energetics of MgFe solid solutions. *Contrib. Mineral. Petrol.*, **145**, 752.
 Geiger, C.A., Armbruster, T., Khomenko, V., Quartieri, S. (2000a): Cordierite I: the coordination of Fe^{2+} . *Am. Mineral.*, **85**, 1255.
 Geiger, C.A., Rager, H., Czank, M. (2000b): Cordierite III: the site occupation and concentration of Fe^{3+} . *Contrib. Mineral. Petrol.*, **140**, 344.
 Goldberg, D.P., Telsler, J., Krzystek, J., Montalban, A.G., Brunel, L.C., Barrett, A.G.M., Hoffman, B.M. (1997): EPR spectra from EPR-silent species: high-field EPR spectroscopy of manganese(III) porphyrins. *J. Am. Chem. Soc.*, **119**, 8722–8723.
 Goldman, D.S., Rossman, G.R., Dollase, W.A. (1977): Channel constituents in cordierite. *Am. Mineral.*, **62**, 1144.
 Green, G.R. & Walker, G. (1985): Luminescence excitation spectra of Mn^{2+} in synthetic forsterite. *Phys. Chem. Miner.*, **12**, 271–278.
 Gunasekaran, S. & Anbalagan, G. (2008): Spectroscopic study of phase transitions in natural calcite mineral. *Spectrochim. Acta A*, **69**, 1246–1251.
 Hedgecock, N.E. & Chakravarty, S.C. (1966): Electron spin resonance of Fe^{+3} in cordierite. *Can. J. Phys.*, **44**, 2749.
 Holmes, O.G. & McClure, D.S. (1957): Optical spectra of hydrated ions of the transition metals. *J. Chem. Phys.*, **26**, 1686–1694.
 Khomenko, V., Langer, K., Geiger, C.A. (2001): Structural locations of the iron ions in cordierite: a spectroscopic study. *Contrib. Mineral. Petrol.*, **141**, 381.
 Krebs, J.J. & Maisch, W.G. (1971): Exchange effects in the optical-absorption spectrum of Fe^{3+} in Al_2O_3 . *Phys. Rev. B*, **4**, 757–769.
 Kuck, S., Hartung, S., Hurling, S., Petermann, K., Huber, G. (1998): Optical transitions in Mn^{3+} -doped garnets. *Phys. Rev. B*, **57**, 2203–2216.
 Lin, L., Min, Y., Chaoshu, S., Weiping, Z., Baogui, Y. (2006): Synthesis and luminescence properties of red phosphors: Mn^{2+} doped MgSiO_3 and Mg_2SiO_4 prepared by sol-gel method. *J. Rare Earths*, **24**, 104–107.
 Lohr Jr., L.L. & McClure, D.S. (1968): Optical spectra of divalent manganese salts. II. The effect of interionic coupling on absorption strength. *J. Chem. Phys.*, **49**, 3516–3521.
 McClure, D.S. (1962): Optical spectra of transition-metal ions in corundum. *J. Chem. Phys.*, **36**, 2757–2779.
 Noginov, M.A., Loutts, G.B., Warren, M. (1999): Spectroscopic studies of Mn^{3+} and Mn^{2+} ions in YAlO_4 . *J. Opt. Soc. Am. B*, **16**, 475–483.
 Padlyak, B., Vlokh, O., Kuklinski, B., Sagoo, K. (2006): Spectroscopy of Mn-doped glasses of $\text{CaO-Ga}_2\text{O}_3\text{-GeO}_2$ system. *Ukr. J. Phys. Opt.*, **7**, 1–10.
 Pollini, I., Spinolo, G., Benedek, G. (1980): Vibrational structure of crystal-field spectra in layered 3d-metal dihalides. *Phys. Rev. B*, **22**, 6369–6390.
 Rakhimov, R.R., Jackson, E.M., Jones, D.E., Loutts, G.B. (2004): Low-field microwave response and electron paramagnetic resonance identification of valence states of manganese including

- octahedral Mn^{5+} in YAlO_3 and CaYAlO_4 . *J. Appl. Phys.*, **95**, 5653–5660.
- Runciman, W.A., Sengupta, D., Gourley, J.T. (1973): The polarized spectra of iron in silicates. II. olivine. *Am. Mineral.*, **58**, 451.
- Sanz-Ortiz, M.N. & Rodríguez, F. (2009): Photoluminescence properties of Jahn-Teller transition-metal ions. *J. Chem. Phys.*, **131**, 124–512.
- Smith, G., Hålenius, U., Langer, K. (1982): Low temperature spectral studies of Mn^{3+} bearing andalusite and epidote type minerals in the range 30000–5000 cm^{-1} . *Phys. Chem. Miner.*, **8**, 136–142.
- Spinolo, G., Fontana, I., Galli, A. (2007): Optical absorption spectra of Fe^{2+} and Fe^{3+} in beryl crystals. *Physica Status Solidi B*, **244**, 4660–4668.
- Stevens, A.L.N. (1979): Red Mn^{2+} luminescence in hexagonal aluminates. *J. Lumin.*, **20**, 99–109.
- Taran, M.N. & Rossman, G.R. (2001): Optical spectroscopic study of tuzualite and a re-examination of the beryl, cordierite, and osumilite spectra. *Am. Mineral.*, **86**, 973.
- van Ipenburg, M.E., Dirksen, G.J., Blasse, G. (1995): Charge-transfer excitation of transition-metal ion luminescence. *Mater. Chem. Phys.*, **39**, 236–238.
- Wertz, J.E. & Bolton, J.R. (1972): Electron spin resonance: elementary theory and practical applications. McGraw-Hill, New York, NY.
- Williams, L.C., Norton, D., Budai, J., Holloway, P.H. (2004): Cathodoluminescence from thin film Zn_2GeO_4 :Mn phosphor grown by pulsed laser deposition. *J. Electrochem. Soc.*, **151**, H188–H191.

Received 17 February 2011

Modified version received 22 July 2011

Accepted 13 December 2011